

Geophysical Research Letters[®]

RESEARCH LETTER

10.1029/2023GL107356

Key Points:

- Short-term inferences of fault coupling provide limited insight into which faults regions can undergo large slip in future earthquakes
- Steady and transient slow slip indicates that fault stress levels are loaded near quasi-static failure conditions
- If a fault region is susceptible to failing dynamically, slow slip may suggest it is critically stressed to fail in a future earthquake

Supporting Information:

Supporting Information may be found in the online version of this article.

Correspondence to:

V. Lambert,
valerelambert@protonmail.ch

Citation:

Lambert, V. (2024). Slow slip as an indicator of fault stress criticality. *Geophysical Research Letters*, 51, e2023GL107356. <https://doi.org/10.1029/2023GL107356>

Received 16 NOV 2023
Accepted 29 APR 2024

Author Contribution:

Conceptualization: Valère Lambert
Formal analysis: Valère Lambert
Methodology: Valère Lambert
Writing – original draft: Valère Lambert

Slow Slip as an Indicator of Fault Stress Criticality

Valère Lambert¹ 

¹Department of Earth and Planetary Sciences, University of California, Santa Cruz, CA, USA

Abstract Fault regions inferred to be slowly slipping are interpreted to accommodate much of tectonic plate motion aseismically and potentially serve as barriers to earthquake rupture. Here, we build on prior work using simulations of earthquake sequences with enhanced dynamic fault weakening to show how fault regions that exhibit decades of steady creep or transient slow-slip events can be driven to dynamically fail by incoming earthquake ruptures. Following substantial earthquake slip, such regions can be under-stressed and locked for centuries prior to slowly slipping again. Our simulations illustrate that slow fault slip indicates that a region is sufficiently loaded to be failing about its quasi-static strength. Hence, if a fault region is susceptible to failing dynamically, then observations of slow slip could serve as an indication that the region is critically stressed and ready to fail in a future earthquake, posing a qualitatively different interpretation of slow slip for seismic hazard.

Plain Language Summary Earthquakes are thought to predominantly occur along sections of faults that appear stuck and actively accumulating strain under tectonic plate motion. Other fault regions observed to be slowly slipping are thought to release some of this strain without causing strong shaking, potentially limiting the location and amount of fault slip in earthquakes. Here we present numerical simulations of long-term fault slip that add to a body of work showing how fault areas can host different styles of slow slip for several decades prior to failing destructively when pushed by an incoming earthquake rupture. Our models show how relatively short-term observations of slow fault slip compared to the recurrence of large earthquakes over several centuries can mask fault regions that are capable of experiencing substantial slip in future earthquakes. Importantly, our simulations suggest that if a fault region is capable of failing during an earthquake, then observations of slow slip may indicate that the region is favorably stressed to fail in a future earthquake, representing a qualitatively different interpretation of slow slip for seismic hazard.

1. Introduction

Determining the maximum plausible earthquake size for a given fault and potential locations of substantial seismic slip are critical components for seismic hazard assessment. Given the relative rarity of large earthquakes, with recurrence times typically greater than a century, such estimates often rely on studying aspects of historical seismicity based on evidence from paleoseismology, tectonic modeling, and historical documentation of earthquake events, when available (Bohnhoff et al., 2016; Cubas et al., 2022; Melnick, 2016; Melgar et al., 2022; Ruiz & Madariaga, 2018; Saillard et al., 2017). However, such historical and geological evidence may not provide conclusive constraints on plausible spatial distributions of seismic slip during great earthquakes, as well as faulting behaviors that occur in between large seismic events.

Geophysical observations are used to infer fault regions that exhibit locking, or negligible motion, versus regions that slowly slip (Bürgmann, 2018). Locked or coupled fault regions are interpreted as areas accumulating elastic strain, which may be released through seismic slip during future earthquakes. Uncoupled or less coupled regions can be inferred to exhibit nearly steady creep and/or transient slow-slip events (SSEs), with regularly occurring SSEs having been inferred across a number of subduction zones as well as along sections of the San Andreas Fault (Michel et al., 2019; Nishikawa et al., 2023; Ozawa et al., 2002; Rogers & Dragert, 2003; Rousset et al., 2019; Schwartz & Rokosky, 2007). As slow-slipping regions accommodate at least part of overall tectonic plate motion aseismically, they may be thought to constrain the amount of seismic slip that can occur in future earthquakes or even act as barriers to earthquake propagation (Rolandone et al., 2018; Saux et al., 2022).

Spatial variations in fault coupling, including the presence of SSEs, are used to inform areas of plausible earthquake slip and models of seismic hazards (Chlieh et al., 2008; Loveless & Meade, 2010; Petersen et al., 2014). Depth variations in fault coupling are used to assess the potential for substantial shallow and deep slip in subduction megathrust earthquakes, which have significant implications for tsunami hazard and on-shore

© 2024, The Author(s).

This is an open access article under the terms of the Creative Commons Attribution-NonCommercial-NoDerivs License, which permits use and distribution in any medium, provided the original work is properly cited, the use is non-commercial and no modifications or adaptations are made.

ground motions, respectively (Ide et al., 2011; Kanamori, 1994; Lay et al., 2012; Simons et al., 2011). For example, the expected down-dip extent of plausible great earthquake scenarios on the Cascadia subduction zone, a critical parameter for shaking in major population centers (Frankel et al., 2018; Wirth & Frankel, 2019), is largely based on inferred interseismic locking contours, with the deepest plausible rupture extent assumed to be limited by regions of regular SSE occurrence (Petersen et al., 2014).

The relationship between SSEs and earthquake hazards remains an important topic of active research, with some observations suggesting SSEs preceding several great subduction events, such as the 2011 M_W 9.0 Tohoku-Oki and 2014 M_W 8.1 Iquique earthquakes (Ito et al., 2013; Kato et al., 2012; Ruiz et al., 2014), as well as earthquake ruptures penetrating into regions known to host slow slip (Lin et al., 2020). A variety of fault models based on low-velocity, laboratory-derived rate-and-state friction laws (e.g. Dieterich, 2007), have reproduced SSEs that sometimes or never transition into dynamic ruptures, often incorporating specific heterogeneity of fault properties, including fault roughness, or slip stabilizing mechanisms that prevent or delay unstable fault slip from accelerating into dynamic rupture (e.g. Cattania & Segall, 2021; Heimisson et al., 2019; N. Kato, 2023; Liu & Rice, 2005, 2007; Liu, 2014; Ozawa et al., 2019; Romanet & Ozawa, 2021; Romanet et al., 2018; Segall & Bradley, 2012; Segall & Rice, 1995; Segall et al., 2010).

Regardless of the capability for slow slip to spontaneously accelerate into dynamic rupture, numerical studies have demonstrated that fault segments that stably creep under slow loading can dynamically fail if they undergo enhanced dynamic weakening when driven to seismic slip rates by an incoming earthquake rupture (Jiang & Lapusta, 2016; Noda & Lapusta, 2013). Such enhanced weakening of fault shear resistance during seismic slip has been hypothesized by theoretical studies (Noda et al., 2009; Rice, 2006; Sibson, 1973), widely documented in laboratory experiments (Acosta et al., 2018; Di Toro et al., 2004; Tsutsumi & Shimamoto, 1997; Wibberley et al., 2008), and shown by numerical studies to reproduce a range of geophysical observations for major plate boundary faults (Lambert, Lapusta, & Faulkner, 2021; Lambert, Lapusta, & Perry, 2021; Perry et al., 2020). The potential for fault regions to become destructive under dynamic loading raises questions about how to interpret observations over periods of slow motion in terms of areas of future earthquake slip.

Here, we build on prior work by Noda and Lapusta (2013) and use numerical simulations of sequences of earthquakes and aseismic slip (SEAS) including enhanced weakening due to the thermal pressurization (TP) of pore fluids to illustrate that fault regions can exhibit extended periods of steady creep and/or SSEs prior to failing dynamically in large earthquakes. Our models show how relatively short-term (decadal-scale) inferences of fault coupling provide limited insight into the longer-term operation of fault segments and regions of potential earthquake slip. Our simulations demonstrate that the presence of slow slip indicates that a given fault region has been loaded to shear stress levels around conditions for quasi-static failure. This result suggests that if a fault region is susceptible to failing dynamically, then observations of slow slip could serve as an indication that these regions are critically stressed and ready to fail in a future earthquake, posing a qualitatively different interpretation of slow slip for potential seismic hazard.

2. Methodology and Model Setup

We utilize numerical methodologies (Lapusta & Liu, 2009; Noda & Lapusta, 2010) that allow us to simulate SEAS in their entirety, including the spontaneous nucleation of slow slip, fully dynamic rupture propagation, postseismic slip, and interseismic periods between seismic events that can last up to tens or hundreds of years and host steady and transient slow slip (Figure 1). Our simulations consider long-term earthquake sequences across two interacting patches along a planar fault governed by rate-and-state friction as well as enhanced dynamic weakening due to the TP of pore fluids (Noda & Lapusta, 2010; Rice, 2006; Sibson, 1973). The fault is embedded in an elastic whole-space and loaded with a long-term tectonic plate rate V_{pl} around 31.54 mm/year (Figure 1a). We further simplify the geometry to consider 2-D simulations of mode II (in-plane) variations in slip on 1-D faults.

The fault models contain two 15-km patches (Figure 1a) separated by a 5-km transition region, and embedded in a velocity-strengthening (VS) domain. Patch A is governed by velocity-weakening (VW) friction at slow slip rates, as well as mild coseismic weakening due to TP. The majority of Patch B is governed by VS friction at slow slip rates and therefore exhibits relatively stable behavior under slow loading. We consider three different fault models (M1-3) that vary the properties of Patch B. In fault model M1, Patch B contains a 3.5-km VW inclusion that is large enough for slip to accelerate 10–1,000 times faster than the long-term slip rate V_{pl} , but not large

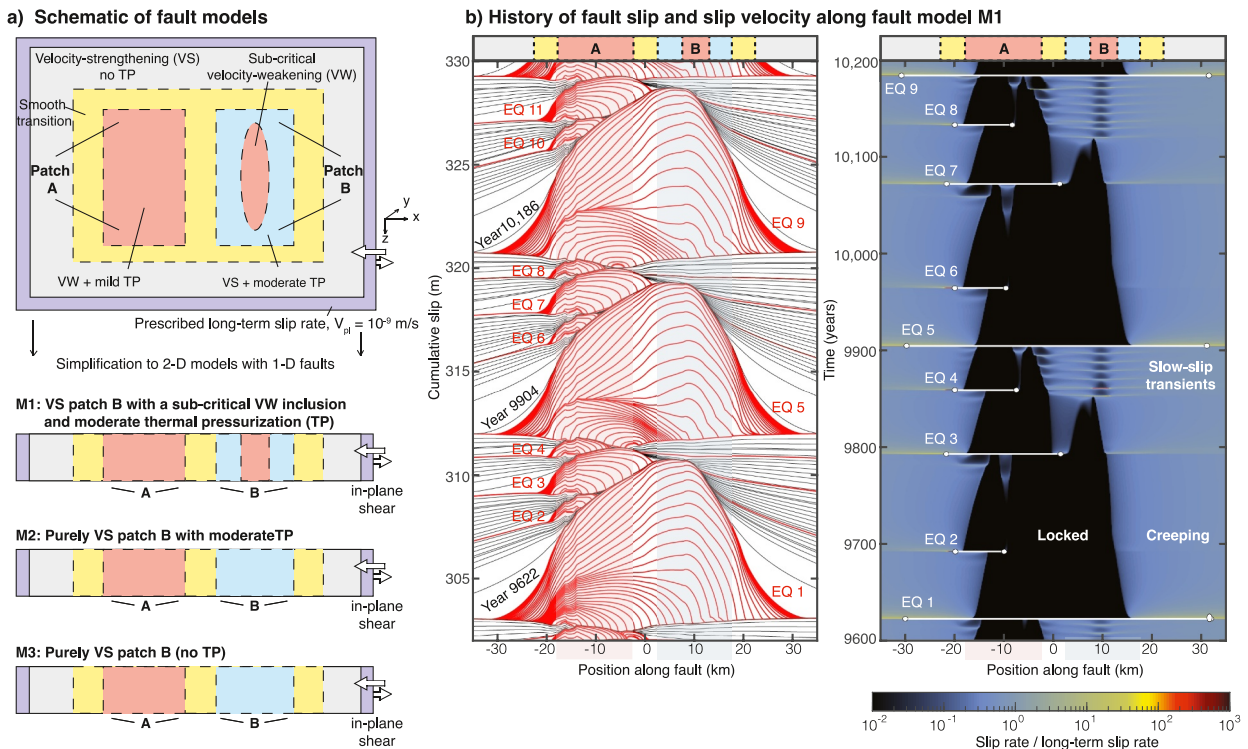


Figure 1. Model schematic and history of slip for two interacting fault patches. (a) Planar fault model with two patches. Patch A is governed by velocity-weakening (VW, red) friction with mild coseismic weakening due to thermal pressurization (TP). Three fault models are considered for Patch B considering as a sub-critical VW patch surrounded by velocity-strengthening (VS) (blue) regions with moderate TP (M1), or purely VS friction, with moderate (M2) or no (M3) TP. (b) Simulated history of fault slip (left) and slip velocity (right) over several earthquake sequences in fault model M1. Individuals earthquakes are denoted by EQ. (Left) Accumulated seismic slip is contoured in red every 0.5 s and shows earthquakes of varying size nucleating in Patch A and sometimes propagating into Patch B. Aseismic slip is contoured in black every 10 years, demonstrating long-term aseismic slip outside of the two patches, as well as in Patch B in between large earthquakes. (Right) The fault slip rate, normalized by the long-term slip rate, over several hundred years demonstrates extended periods of locking (black) following earthquake ruptures (indicated by white lines) in Patches A and B. Creep (blue) penetrates into the locked patches, resulting in earthquake nucleation in Patch A and periods of repeating slow-slip transients in Patch B.

enough to nucleate dynamic ruptures. We refer to this VW inclusion as sub-critical to denote that the VW region is smaller than the critical dimension for dynamic rupture nucleation under slow loading (Figure 1b, Text S1 in Supporting Information S1; Dal Zilio et al., 2020; Liu & Rice, 2005). For fault models M2 and M3, Patch B is governed by purely VS friction. Patch B is susceptible to moderate coseismic weakening due to TP in models M1 and M2, but not in model M3.

The model setup and parameters are largely inspired by the models of Noda and Lapusta (2013), motivated by laboratory measurements of frictional and transport properties from samples taken from shallow boreholes in the Chelengpu fault, Taiwan, which hosted the 1,999 M_w 7.6 Chi-Chi earthquake (Tanikawa & Shimamoto, 2009). Specifically, the samples suggest spatial heterogeneity in VW and VS properties between regions of earthquake nucleation and later rupture propagation, respectively. Importantly, the samples that exhibited VS behavior under slow sliding were proposed to be more susceptible to dramatic weakening at seismic slip rates, such as from TP, as has been also noted by other experimental studies of clay-rich fault gouges, which are prevalent on mature faults (Faulkner et al., 2011). Comparable model geometries (in 3D) and conditions were used to reproduce several aspects of the 2011 M_w 9.0 Tohoku-oki earthquake, where substantial co-seismic slip was driven through the shallow megathrust, which had been considered to be previously creeping (Ide et al., 2011; Noda & Lapusta, 2013; Simons et al., 2011).

Here, we do not aim to match specific observations from a particular fault setting but use our models to explore the relationship between slow fault slip, dynamic weakening, and fault stress state. VW Patch A can be taken to reflect a typical fault seismogenic region, where earthquakes can nucleate and grow. Our models do not include a

free surface, hence Patch B could reflect deeper or shallower fault extents that host slow slip and neighbor the seismogenic zone, such as for a megathrust fault (e.g. Lay et al., 2012), or lateral variations in properties and coupling along a transform fault, such as around the creeping section of the San Andreas Fault (Jolivet et al., 2015). In order to focus on fault regions that exhibit steady and transient slow slip and their response to dynamic loading, properties of Model M1 are chosen to produce regularly recurring SSEs in Patch B that do not nucleate into dynamic events. Further description of the model ingredients and numerical methodology is given (Table S1 in Supporting Information S1).

3. Modeling Results

Our simulations of fault model M1 reveal a rich history of fault slip over long-term earthquake sequences. Earthquake ruptures of differing size nucleate in Patch A and sometimes propagate into Patch B during large events roughly every 250–300 years (Figure 1b). Both Patches A and B exhibit periods of locking following coseismic slip. Over the interseismic period between large events, creep penetrates into both locked patches, leading to the nucleation of several smaller earthquakes in Patch A that fail to propagate into Patch B and sometimes only rupture part of Patch A. Patch B remains locked for a longer period than Patch A due to the greater coseismic slip in Patch B versus A during large events, which results in part from the differing efficiencies of dynamic weakening from TP (Figure 1b). Creep eventually propagates into Patch B later in the interseismic period, leading to the regular occurrence of SSEs (roughly every 10 years) along the sub-critical VW inclusion over the 50–100 years prior to subsequent large events. Similar long-term behavior is observed in fault model M2, with earthquakes nucleating in Patch A and sometimes propagating into Patch B (Figure S1 in Supporting Information S1). However, without the sub-critical VW inclusion in model M2, Patch B exhibits nearly steady interseismic creep after locking, as observed in the models of Noda and Lapusta (2013).

Let us consider the slip behavior leading up to large earthquakes in our different fault models M1–3. We can examine the interseismic slip that accumulates over the fault throughout the 40-year period prior to large earthquakes, compared to the expected slip over this period given the long-term plate rate (Figure 2a). Over this period we see that Patch A, which is locked, exhibits a notable deficit in accumulated interseismic slip. However, outside of Patch A, the distribution of accumulated interseismic slip becomes more consistent with that expected at the long-term plate rate, with some reduced interseismic creep consistent with stress shadowing from the locked Patch A (e.g. Hetland & Simons, 2010; Lindsey et al., 2021). No remarkable slip deficit is shown over Patch B, which either creeps or exhibit SSEs during this period. In fact, we see that the 40-year interseismic slip-deficit distributions prior to large earthquakes for all three fault models M1–3 can appear virtually indistinguishable (yellow vs. gray and black contours in Figure 2a). However, the subsequent large earthquakes are notably different. Large earthquakes in fault models M1 and M2 rupture into Patch B with moderate TP, resulting in larger rupture sizes and slip compared to ruptures in fault model M3 without TP in Patch B, which are mostly confined to Patch A (Figures 2c and 2d, Figure S2 in Supporting Information S1). Moreover, despite most of the 40-year interseismic slip deficit occurring in Patch A, the peak coseismic slip for large earthquakes occurs in Patch B for models M1 and M2 with moderate TP (Figures 2a–2c, Noda & Lapusta, 2013).

We find that we are not able to reliably distinguish between fault regions in our models that will host large coseismic slip based on the accumulated slip deficit during the later interseismic periods. In our fault models, Patch B can creep or exhibit regular SSEs over several decades, accommodating most of the expected long-term plate motion over this period and accumulating several meters of slip aseismically (Figures 1b, 3, and 4, Figure S1 in Supporting Information S1). The same patch can then experience 5–10 m of seismic slip during large earthquakes and be subsequently locked for hundreds of years. In fact, the majority of the long-term plate motion over thousands of years for Patch B in fault models M1 and M2 is accommodated by seismic slip during great earthquakes (Figure 1b and Figure S1 in Supporting Information S1), which would be obscured by observations limited to the decades of slow slip during the late interseismic period (Figure 2a).

The variations in fault coupling in our models (defined as $1 - V/V_{pl}$ when $V \leq V_{pl}$ and 0 when $V \geq V_{pl}$, as in Noda & Lapusta, 2013) reflect the evolution of local fault stress over sequences of earthquakes (Figures 3–4 and Figure 3 in Supporting Information S1). Following earthquake ruptures, locking, or increased coupling, along fault regions that experienced substantial coseismic slip corresponds to the segments being under-stressed with respect to their local quasi-static strength $\tau_{ss}(V_{pl})$ due to the coseismic stress drop (Figures 3b, 3c, 4b, and 4c, Figure S3 in Supporting Information S1). Here, we consider a representative value of the local quasi-static fault strength

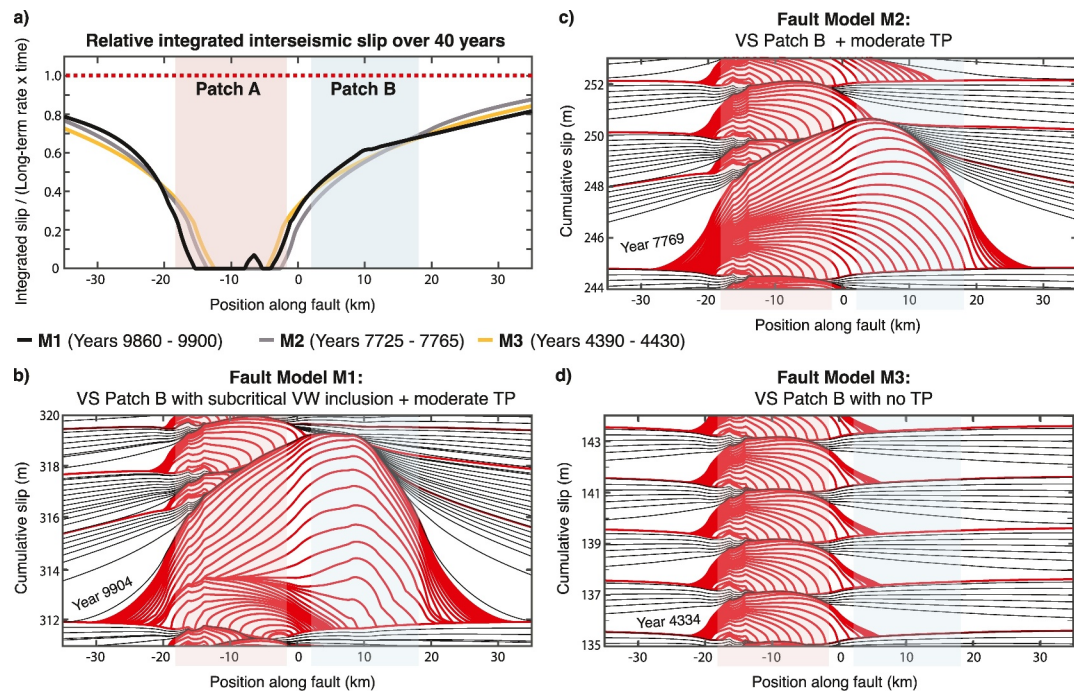


Figure 2. Limited correlation between regions of large coseismic slip and short-term interseismic slip distributions. (a) Virtually identical distributions of interseismic slip accumulated over 40 years prior to large earthquakes in fault models M1–3, relative to the expected slip at the long-term plate rate. An accumulated slip deficit is shown in Patch A, which is locked prior to the earthquake, but no remarkable deficit is shown in Patch B over the 40-year period. (b–d) Differing distributions of coseismic slip (red contours every 0.5 s) during large earthquakes following the corresponding interseismic period shown in (a). Large earthquakes in fault models M1 and M2 with moderate thermal pressurization (TP) in Patch B (b, c) exhibit larger rupture sizes and slip compared to ruptures in fault model M3 without TP in Patch B (d), which are mostly confined to Patch A. Despite most of the 40-year interseismic slip deficit occurring in Patch A, the peak coseismic slip for large earthquakes occurs in Patch B for models M1 and M2 with moderate TP (b, c).

defined as the shear resistance under steady-state creep at the long-term plate rate τ_{ss} (V_{pl}), which has been found to be comparable to the average prestress consistent with rupture nucleation in previous numerical studies (Lambert, Lapusta, & Faulkner, 2021, Text S1 in Supporting Information S1). Following coseismic slip in large earthquakes, Patch B can be locked and under-stressed for several hundred years, with smaller earthquakes in Patch A failing to penetrate substantially into Patch B, due in part to the low stress conditions (Figure 3). Regions in Patch B are eventually reloaded toward their local quasi-static strength, which is when the regions begin to creep and exhibit SSEs again (Figures 3b, 3c, 4b, and 4c).

Steady creep and SSEs occur in Patch B when the shear stress conditions along the fault have been loaded to quasi-static failure, which is indicative of the mid-to-late interseismic period between great earthquakes in fault models M1 and M2 (Figures 3c and 4c). Simulated SSEs in fault model M1 exhibit stress drops between 10 and 100 kPa, comparable to those of natural SSEs, which are typically several orders of magnitude lower than static stress drops inferred from natural earthquakes (Gao et al., 2012). The shear stress changes in our models during SSEs thus represent relatively small deviations in shear stress about the quasi-static fault strength (Figure 3c).

For fault model M1, SSEs in Patch B never spontaneously transition into dynamic events. The SSEs in Patch B are influenced by stress transfer from earthquakes in Patch A, with small earthquakes triggering more pronounced slip acceleration (e.g., around year 9,860 in Figure 3b), and could potentially self-nucleate or be triggered to accelerate into dynamic ruptures with slightly different fault properties or geometry for Patch B. Such SSEs that transition into dynamic events may or may not be distinguishable from preceding SSEs that do not (e.g. Segall & Bradley, 2012). In our fault models, SSEs or transient periods of decreased coupling also occur within the nucleation region of earthquakes in Patch A prior to dynamic events (Figures 3a and 4a). Such behavior has been noted in prior numerical studies, indicating the progressive loading of the locked VW region, and the continued acceleration of slip and failed nucleation of dynamic rupture due to lower shear stress conditions ahead of the slip

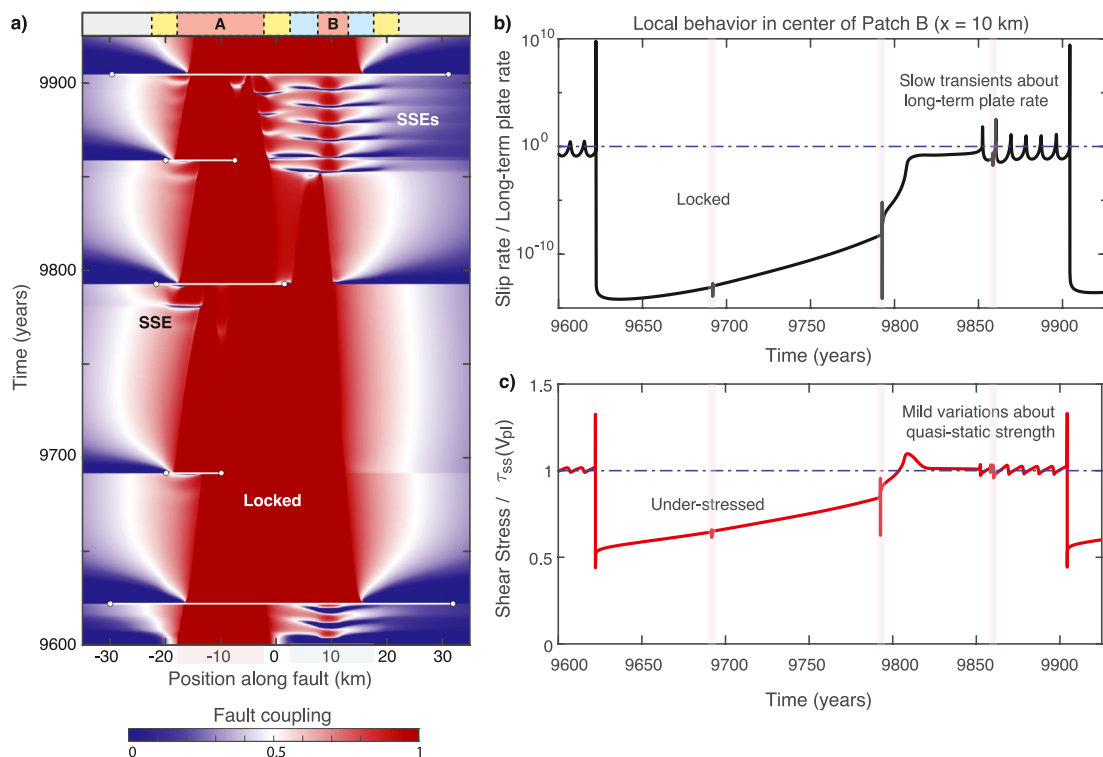


Figure 3. Fault coupling and shear stress evolution between two large earthquakes in fault model M1. (a) Evolution of fault coupling, with locked segments corresponding to a coupling of one. White lines indicate the extent of earthquake ruptures. (b, c) Evolution of local slip rate and shear stress in the center of Patch B ($x = 10$ km). (b) Patch B is initially locked following large coseismic slip, then begins to creep and exhibit regular slow-slip events (SSEs) over several decades preceding the next large earthquake. (c) Locking in Patch B corresponds to the region being substantially under-stressed with respect to the quasi-static strength $\tau_{ss}(V_p)$. Patch B is eventually reloaded and exhibits SSEs, which represent relatively mild changes in shear stress about the quasi-static strength. Pink shading denotes the timing of earthquakes in Patch A that fail to propagate into Patch B.

front (e.g. N. Kato, 2023; Lambert, Lapusta, & Faulkner, 2021). These results show that the occurrence of slow slip in different regions of our fault models that can participate in earthquake slip indicates that these regions are approaching favorable stress conditions to participate in a future earthquake, regardless of whether the local fault properties support earthquake nucleation.

3.1. Discussion and Conclusions

Our simulation results illustrate the challenge of distinguishing between fault regions that are capable of undergoing large seismic slip during earthquakes given a limited observational period of fault coupling compared to the potentially great variability in fault behavior over centuries or millenia spanning several great earthquakes (Figure 2). Moreover, our results emphasize the importance of considering the potential for dynamic overshoot with regards to long-term kinematic consistency of fault motion, as suggested for the 2011 $M_W 9.0$ Tohoku-oki earthquake (e.g. Ide et al., 2011). The seismic potential of a fault region is regularly thought to accommodate an interseismic slip deficit accumulated prior to rupture. However, fault regions can be dynamically driven to undergo substantial slip due to the strain energy released by other slipping regions during an earthquake rupture, regardless of the degree of prior local coupling (Ito et al., 2013; Jiang & Lapusta, 2016; Noda & Lapusta, 2013). Such dynamic overshoot would result in the region being subsequently under-stressed, and hence locked, for some period to account for the coseismic slip (Figures 3 and 4).

Our results demonstrate that if a fault region is susceptible to failing dynamically during earthquake ruptures, then the presence of slow slip could indicate that the region has been loaded to quasi-static failure, and thus is favorably stressed to fail in a future earthquake. Such result could present a qualitatively different interpretation of slow slip and low fault coupling for seismic hazard compared to traditional considerations. This is not to say that all fault segments that host slow slip will fail during impending earthquakes, even if they are susceptible to dynamic

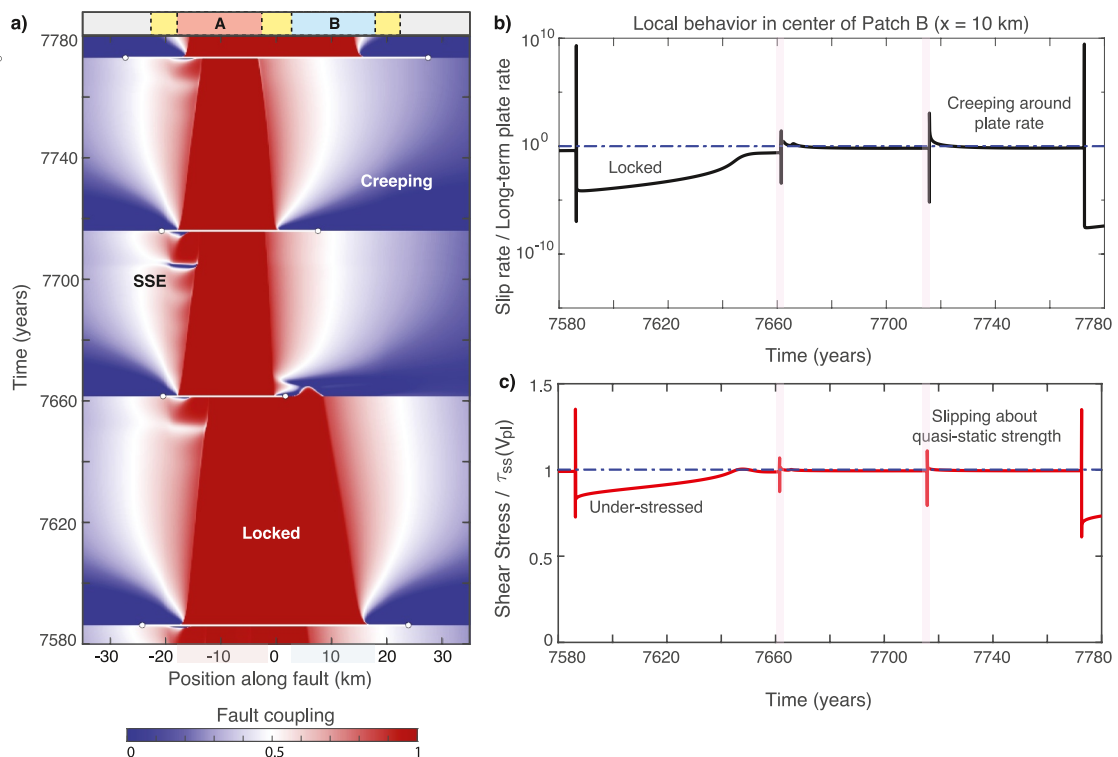


Figure 4. Fault coupling and shear stress evolution between two large earthquakes in fault model M2. (a) Evolution of fault coupling, with locked segments corresponding to a coupling of one. White lines indicate the extent of earthquake ruptures. (b, c) Evolution of local slip rate and shear stress in the center of Patch B ($x = 10$ km). (b) Similar to fault model M1, Patch B is initially locked following substantial coseismic slip, then begins to creep nearly steadily around the long-term plate rate for over 100 years prior to slipping in the next large earthquake. Pink shading denotes the timing of smaller earthquakes in Patch A that fail to substantially propagate into Patch B and (c) Locking in Patch B corresponds to the region being under-stressed with respect to the local quasi-static strength $\tau_{ss}(V_{pl})$. Patch B is eventually reloaded and creeps nearly steadily about $\tau_{ss}(V_{pl})$.

weakening. The processes governing whether patch B undergoes seismic slip in our fault models depends on a number of factors, including the local properties and susceptibility to dynamic fault weakening (e.g., Models M2 vs. M3), the characteristics of the incoming dynamic rupture, and the prestress state of the patch prior to rupture (Figures 3 and 4).

The principle conclusion of this work is that observations of steady or transient slow slip can indicate that the current local fault stress state is near conditions for quasi-static failure, or that the region is critically stressed under slow loading. We expect this result to be consistent among different models of slow-slip propagation, given the relatively mild static stress changes and stress transfer expected to be driving slip propagation in SSEs compared to dynamic rupture. The proposition that slow fault slip can serve as an indicator of relative fault stress follows from the mechanical argument that locked fault regions are under-stressed with respect to conditions for quasi-static failure, typically interpreted as the fault's quasi-static (or static) strength. Fault regions that are creeping or slowly failing may then be interpreted to be sufficiently stressed to be yielding about the quasi-static strength (Figures 3 and 4 and Figure S3b in Supporting Information S1).

The interpretation that the local fault stress state is close to quasi-static failure for slow slip is consistent with laboratory experiments and numerical studies showing increased slow slip and foreshock activity leading up to earthquake nucleation (Cattania & Segall, 2021; Lambert, Lapusta, & Faulkner, 2021; Marty et al., 2023; McLaskey, 2019; N. Kato, 2023; Romanet & Ozawa, 2021), as well as observations suggesting that slow-slip transients and associated tremor activity can be sensitive to small external stress perturbations, such as tidal forcing and changes in ocean water column (Gomberg et al., 2020; Hawthorne & Rubin, 2010; Houston, 2015; Ide, 2010; Royer et al., 2015; Shelly et al., 2007; Tanaka et al., 2015). SSEs occur as failed earthquakes in our models due to both persistent heterogeneity in fault properties, like the sub-critical VW region in Patch B for Model M1, as well as transient shear stress heterogeneity in Patch A due to prior earthquake slip (Figures 3a and

4a), consistent with prior studies (e.g. Liu & Rice, 2005; N. Kato, 2023). In both cases, SSEs indicate that the local shear stress is near the local quasi-static strength allowing slip to accelerate. Whether the SSEs transition into dynamic rupture in our models depends on if the accelerated slipping region is sufficiently large to release enough stored energy to radiate waves (Dal Zilio et al., 2020; Liu & Rice, 2005), which depends on the fault properties and conditions within and ahead of the slipping region. The SSEs may eventually transition into dynamic rupture (as in Patch A), or persist as quasi-periodic SSEs that never spontaneously nucleate into earthquakes (as in Patch B). Importantly, our modeling demonstrates that slow slip phenomena are not only relevant for assessing conditions surrounding earthquake nucleation, but may also inform the stress conditions over fault regions in which ruptures may dynamically propagate.

Such interpretation of slow fault slip can be an important consideration for examining the potential rupture extent of future large earthquakes, including possible rupture propagation into shallow and deep fault regions that actively host slow slip (Nishikawa et al., 2023; Rolandone et al., 2018; Saux et al., 2022). For example, fault coupling models, including regions of low coupling, can help inform the initial stress conditions for exploring detailed dynamic rupture simulations of plausible earthquake scenarios with realistic fault geometries, including consideration of varying efficiencies of dynamic fault weakening (e.g. Ulrich et al., 2019).

Our results add to a body of work suggesting that the seismic potential of a fault depends not only on the stability conditions under slow loading and coupling prior to rupture, but how the region responds to dynamic loading from incoming earthquake ruptures, including the potential for enhanced dynamic fault weakening (Jiang & Lapusta, 2016; Noda & Lapusta, 2013). Dynamic failure in our fault models is predominantly controlled by fault weakening due to the TP of pore fluids, however the relationship between changes in fault coupling and relative stress conditions are expected to be consistent for other mechanisms of dynamic fault failure. In particular, studies considering more realistic dipping fault geometries of subduction megathrusts have shown that a number of mechanisms can lead to enhanced slip in the shallow megathrust besides strong coseismic weakening of fault shear resistance, including dynamic rupture in the presence of reduced fault confinement, weaker and more compliant sediments, and wave-mediated interactions with the free surface (e.g. Brune, 1996; Gabuchian et al., 2017; Lotto et al., 2017; Ma & Hirakawa, 2013; Ma & Nie, 2019; Oglesby et al., 2000; Yin & Denolle, 2021).

The array of potentially favorable mechanisms and conditions for dynamic failure of the shallow megathrust raises the question as to why shallow slip does not occur more regularly during megathrust earthquakes. One explanation would be that structural and/or constitutive features of the subduction toe sufficiently dissipates energy from incoming ruptures to prohibit notable shallow seismic slip. Further work is warranted to discern the susceptibility of different fault regions to failing dynamically during large earthquakes, including assessing the potential for enhanced dynamic weakening and how efficiently strain energy released during incoming dynamic ruptures may be dissipated. Improved constraints on fault zone structure, such as from seismic imaging, as well as insight from geology and laboratory experiments can be coupled with numerical modeling efforts to discern appropriate-scaled constitutive behaviors of fault zone materials as well as how deformation is partitioned across fault zone structures during dynamic rupture scenarios. Geodetic measurements, including from seafloor geodesy, may also assist in constraining transient aspects of fault zone rheology in response to different stress perturbations, such as from tides as well as regional and distant earthquakes. Importantly, such efforts would advocate for continuous geodetic measurements in order to resolve transient deformation processes.

Another possibility is that considerable shallow slip does occur during great megathrust earthquakes, leaving the shallower sections of the megathrust substantially under-stressed and limiting the rupture extent of more moderate-sized events in between great earthquakes (Figures 3 and 4). In such case, our modeling results suggest that observations of shallow slow slip would indicate that the shallow megathrust has been sufficiently reloaded and is potentially ready to dynamically fail again.

Data Availability Statement

Data from numerical simulations related to this paper are available at Lambert (2023).

Acknowledgments

The numerical simulations for this work were conducted on the lux supercomputer at UC Santa Cruz, funded by NSF MRI Grant AST 1828315, and the Bridges-2 supercomputer at the Pittsburgh Supercomputing Center (ACCESS Allocation EES230068). V.L. thanks Rishav Mallick, Heather Savage, Thorne Lay, Kelian Dascher-Cousineau, Pierre Romanet, Germán Prieto and an anonymous reviewer for helpful discussions and review of the manuscript.

References

- Acosta, M., Passelègue, F. X., Schubnel, A., & Violay, M. (2018). Dynamic weakening during earthquakes controlled by fluid thermodynamics. *Nature Communications*, 9(1), 3074. <https://doi.org/10.1038/s41467-018-05603-9>
- Bohnhoff, M., Martínez-Garzón, P., Bulut, F., Stierle, E., & Ben-Zion, Y. (2016). Maximum earthquake magnitudes along different sections of the North Anatolian fault zone. *Tectonophysics*, 674, 147–165. <https://doi.org/10.1016/j.tecto.2016.02.028>
- Brune, J. N. (1996). Particle motions in a physical model of shallow angle thrust faulting. *Proceedings of the Indian Academy of Sciences - Earth & Planetary Sciences*, 105(2), 197–206. <https://doi.org/10.1007/BF02876014>
- Bürgmann, R. (2018). The geophysics, geology and mechanics of slow fault slip. *Earth and Planetary Science Letters*, 495, 112–134. <https://doi.org/10.1016/j.epsl.2018.04.062>
- Cattania, C., & Segall, P. (2021). Precursory slow slip and foreshocks on rough faults. *Journal of Geophysical Research: Solid Earth*, 126(4), e2020JB020430. <https://doi.org/10.1029/2020JB020430>
- Chlieh, M., Avouac, J. P., Sieh, K., Natawidjaja, D. H., & Galetzka, J. (2008). Heterogeneous coupling of the Sumatran megathrust constrained by geodetic and paleogeodetic measurements. *Journal of Geophysical Research*, 113(B5), B05305. <https://doi.org/10.1029/2007JB004981>
- Cubas, N., Agard, P., & Tissandier, R. (2022). Earthquake ruptures and topography of the Chilean margin controlled by plate interface deformation. *Solid Earth*, 13(3), 779–792. <https://doi.org/10.5194/se-13-779-2022>
- Dal Zilio, L., Lapusta, N., & Avouac, J.-P. (2020). Unraveling scaling properties of slow-slip events. *Geophysical Research Letters*, 47(10), e2020GL087477. <https://doi.org/10.1029/2020GL087477>
- Dieterich, J. H. (2007). Applications of rate- and state-dependent friction to models of fault slip and earthquake occurrence. In G. Schubert (Ed.), *Treatise on geophysics* (pp. 107–129). Elsevier. <https://doi.org/10.1016/B978-044452748-6.00065-1>
- Di Toro, G., Goldsby, D. L., & Tullis, T. E. (2004). Friction falls towards zero in quartz rock as slip velocity approaches seismic rates. *Nature*, 427(6973), 436–439. <https://doi.org/10.1038/nature02249>
- Faulkner, D. R., Mitchell, T. M., Behnson, J., Hirose, T., & Shimamoto, T. (2011). Stuck in the mud? Earthquake nucleation and propagation through accretionary forearcs. *Geophysical Research Letters*, 38(18), L18303. <https://doi.org/10.1029/2011GL048552>
- Frankel, A., Wirth, E., Marafi, N., Vidale, J., & Stephenson, W. (2018). Broadband synthetic seismograms for magnitude 9 Earthquakes on the Cascadia megathrust based on 3D simulations and stochastic synthetics, Part 1: Methodology and overall results. *Bulletin of the Seismological Society of America*, 108(5A), 2347–2369. <https://doi.org/10.1785/0120180034>
- Gabuchian, V., Rosakis, A. J., Bhat, H. S., Madariaga, R., & Kanamori, H. (2017). Experimental evidence that thrust earthquake ruptures might open faults. *Nature*, 545(7654), 336–339. <https://doi.org/10.1038/nature22045>
- Gao, H., Schmidt, D. A., Weldon, I., & Ray, J. (2012). Scaling relationships of source parameters for slow slip events. *Bulletin of the Seismological Society of America*, 102(1), 352–360. <https://doi.org/10.1785/01201110096>
- Gomberg, J., Baxter, P., Smith, E., Ariyoshi, K., & Chiswell, S. M. (2020). The ocean's impact on slow slip events. *Geophysical Research Letters*, 47(14), e2020GL087273. <https://doi.org/10.1029/2020GL087273>
- Hawthorne, J. C., & Rubin, A. M. (2010). Tidal modulation of slow slip in Cascadia. *Journal of Geophysical Research*, 115(B9), B09406. <https://doi.org/10.1029/2010JB007502>
- Heimisson, E. R., Dunham, E. M., & Almquist, M. (2019). Poroelastic effects destabilize mildly rate-strengthening friction to generate stable slow slip pulses. *Journal of the Mechanics and Physics of Solids*, 130, 262–279. <https://doi.org/10.1016/j.jmps.2019.06.007>
- Hetland, E. A., & Simons, M. (2010). Post-seismic and interseismic fault creep ii: Transient creep and interseismic stress shadows on megathrusts. *Geophysical Journal International*, 181(1), 99–112. <https://doi.org/10.1111/j.1365-246X.2009.04482.x>
- Houston, H. (2015). Low friction and fault weakening revealed by rising sensitivity of tremor to tidal stress. *Nature Geoscience*, 8(5), 409–415. <https://doi.org/10.1038/ngeo2419>
- Ide, S. (2010). Striations, duration, migration and tidal response in deep tremor. *Nature*, 466(7304), 356–359. <https://doi.org/10.1038/nature09251>
- Ide, S., Baltay, A., & Beroza, G. C. (2011). Shallow dynamic overshoot and energetic deep rupture in the 2011 Mw 9.0 Tohoku-Oki Earthquake. *Science*, 332(6036), 1426–1429. <https://doi.org/10.1126/science.1207020>
- Ito, Y., Hino, R., Kido, M., Fujimoto, H., Osada, Y., Inazu, D., et al. (2013). Episodic slow slip events in the Japan subduction zone before the 2011 Tohoku-Oki earthquake. *Tectonophysics*, 600, 14–26. <https://doi.org/10.1016/j.tecto.2012.08.022>
- Jiang, J., & Lapusta, N. (2016). Deeper penetration of large earthquakes on seismically quiescent faults. *Science*, 352(6291), 1293–1297. <https://doi.org/10.1126/science.aaf1496>
- Jolivet, R., Simons, M., Agram, P. S., Duputel, Z., & Shen, Z.-K. (2015). Aseismic slip and seismogenic coupling along the central San Andreas Fault. *Geophysical Research Letters*, 42(2), 297–306. <https://doi.org/10.1002/2014GL062222>
- Kanamori, H. (1994). Mechanics of Earthquakes. *Annual Review of Earth and Planetary Sciences*, 22(1), 207–237. <https://doi.org/10.1146/annurev.ea.22.050194.001231>
- Kato, A., Obara, K., Igarashi, T., Tsuruoka, H., Nakagawa, S., & Hirata, N. (2012). Propagation of slow slip leading up to the 2011 Mw 9.0 Tohoku-Oki Earthquake. *Science*, 335(6069), 705–708. <https://doi.org/10.1126/science.1215141>
- Kato, N. (2023). Numerical simulation of episodic aseismic slip events as incomplete nucleation of seismic slip due to heterogeneous stress distribution. *Bulletin of the Seismological Society of America*, 113(5), 2009–2025. <https://doi.org/10.1785/0120230048>
- Lambert, V. (2023). Slow slip as an indicator of fault stress criticality [Dataset]. Zenodo. <https://doi.org/10.5281/zenodo.10126627>
- Lambert, V., Lapusta, N., & Faulkner, D. (2021). Scale dependence of earthquake rupture prestress in models with enhanced weakening: Implications for event statistics and inferences of fault stress. *Journal of Geophysical Research: Solid Earth*, 126(10), e2021JB021886. <https://doi.org/10.1029/2021JB021886>
- Lambert, V., Lapusta, N., & Perry, S. (2021). Propagation of large earthquakes as self-healing pulses or mild cracks. *Nature*, 591(7849), 252–258. <https://doi.org/10.1038/s41586-021-03248-1>
- Lapusta, N., & Liu, Y. (2009). Three-dimensional boundary integral modeling of spontaneous Earthquake sequences and aseismic slip. *Journal of Geophysical Research*, 114(B9), B09–B303. <https://doi.org/10.1029/2008JB005934>
- Lay, T., Kanamori, H., Ammon, C. J., Koper, K. D., Hutko, A. R., Ye, L., et al. (2012). Depth-varying rupture properties of subduction zone megathrust faults. *Journal of Geophysical Research*, 117(B4), B04311. <https://doi.org/10.1029/2011JB009133>
- Lin, J.-T., Aslam, K. S., Thomas, A. M., & Melgar, D. (2020). Overlapping regions of coseismic and transient slow slip on the Hawaiian décollement. *Earth and Planetary Science Letters*, 544, 316–335. <https://doi.org/10.1016/j.epsl.2020.116353>
- Lindsey, E. O., Mallick, R., Hubbard, J. A., Bradley, K. E., Almeida, R. V., Moore, J. D. P., et al. (2021). Slip rate deficit and earthquake potential on shallow megathrusts. *Nature Geoscience*, 14(5), 321–326. <https://doi.org/10.1038/s41561-021-00736-x>
- Liu, Y. (2014). Source scaling relations and along-strike segmentation of slow slip events in a 3-D subduction fault model. *Journal of Geophysical Research: Solid Earth*, 119(8), 6512–6533. <https://doi.org/10.1002/2014JB011144>

- Liu, Y., & Rice, J. R. (2005). Aseismic slip transients emerge spontaneously in three-dimensional rate and state modeling of subduction Earthquake sequences. *Journal of Geophysical Research*, 110(B8), B08307. <https://doi.org/10.1029/2004JB003424>
- Liu, Y., & Rice, J. R. (2007). Spontaneous and triggered aseismic deformation transients in a subduction fault model. *Journal of Geophysical Research*, 112(B9), B09404. <https://doi.org/10.1029/2007JB004930>
- Lotto, G. C., Dunham, E. M., Jeppson, T. N., & Tobin, H. J. (2017). The effect of compliant prisms on subduction zone earthquakes and tsunamis. *Earth and Planetary Science Letters*, 458, 213–222. <https://doi.org/10.1016/j.epsl.2016.10.050>
- Loveless, J. P., & Meade, B. J. (2010). Geodetic imaging of plate motions, slip rates, and partitioning of deformation in Japan. *Journal of Geophysical Research*, 115(B2), B02410. <https://doi.org/10.1029/2008JB006248>
- Ma, S., & Hirakawa, E. T. (2013). Dynamic wedge failure reveals anomalous energy radiation of shallow subduction Earthquakes. *Earth and Planetary Science Letters*, 375, 113–122. <https://doi.org/10.1016/j.epsl.2013.05.016>
- Ma, S., & Nie, S. (2019). Dynamic wedge failure and along-arc variations of tsunamigenesis in the Japan Trench margin. *Geophysical Research Letters*, 46(15), 8782–8790. <https://doi.org/10.1029/2019GL083148>
- Marty, S., Schubnel, A., Bhat, H. S., Aubry, J., Fukuyama, E., Latour, S., et al. (2023). Nucleation of laboratory earthquakes: Quantitative analysis and scalings. *Journal of Geophysical Research: Solid Earth*, 128(3), e2022JB026294. <https://doi.org/10.1029/2022JB026294>
- McLaskey, G. C. (2019). Earthquake initiation from laboratory observations and implications for foreshocks. *Journal of Geophysical Research: Solid Earth*, 124(12), 12882–12904. <https://doi.org/10.1029/2019JB018363>
- Melgar, D., Sahakian, V. J., & Thomas, A. M. (2022). Deep coseismic slip in the Cascadia megathrust can be consistent with coastal subsidence. *Geophysical Research Letters*, 49(3), e2021GL097404. <https://doi.org/10.1029/2021GL097404>
- Melnick, D. (2016). Rise of the central Andean coast by Earthquakes straddling the Moho. *Nature Geoscience*, 9(5), 401–407. <https://doi.org/10.1038/ngeo2683>
- Michel, S., Gualandi, A., & Avouac, J.-P. (2019). Interseismic coupling and slow slip events on the Cascadia megathrust. *Pure and Applied Geophysics*, 176(9), 3867–3891. <https://doi.org/10.1007/s00420-018-1991-x>
- Nishikawa, T., Ide, S., & Nishimura, T. (2023). A review on slow Earthquakes in the Japan Trench. *Progress in Earth and Planetary Science*, 10(1), 1. <https://doi.org/10.1186/s40645-022-00528-w>
- Noda, H., Dunham, E. M., & Rice, J. R. (2009). Earthquake ruptures with thermal weakening and the operation of major faults at low overall stress levels. *Journal of Geophysical Research*, 114(B7), B07302. <https://doi.org/10.1029/2008JB006143>
- Noda, H., & Lapusta, N. (2010). Three-dimensional earthquake sequence simulations with evolving temperature and pore pressure due to shear heating: Effect of heterogeneous hydraulic diffusivity. *Journal of Geophysical Research*, 115(B12), B123–B141. <https://doi.org/10.1029/2010JB007780>
- Noda, H., & Lapusta, N. (2013). Stable creeping fault segments can become destructive as a result of dynamic weakening. *Nature*, 493(7433), 518–521. <https://doi.org/10.1038/nature11703>
- Oglesby, D. D., Archuleta, R. J., & Nielsen, S. B. (2000). Dynamics of dip-slip faulting: Explorations in two dimensions. *Journal of Geophysical Research*, 105(B6), 13643–13653. <https://doi.org/10.1029/2000JB900055>
- Ozawa, S., Murakami, M., Kaidzu, M., Tada, T., Sagiyama, T., Hatanaka, Y., et al. (2002). Detection and monitoring of ongoing aseismic slip in the Tokai region, central Japan. *Science*, 298(5595), 1009–1012. <https://doi.org/10.1126/science.1076780>
- Ozawa, S. W., Hatano, T., & Kame, N. (2019). Longer migration and spontaneous decay of aseismic slip pulse caused by fault roughness. *Geophysical Research Letters*, 46(2), 636–643. <https://doi.org/10.1029/2018GL081465>
- Perry, S. M., Lambert, V., & Lapusta, N. (2020). Nearly magnitude-invariant stress drops in simulated crack-like earthquake sequences on rate-and-state faults with thermal pressurization of pore fluids. *Journal of Geophysical Research: Solid Earth*, 125(3), e2019JB018597. <https://doi.org/10.1029/2019JB018597>
- Petersen, M. D., Moschetti, M. P., Powers, P. M., Mueller, C. S., Haller, K. M., Frankel, A. D., et al. (2014). Documentation for the 2014 update of the United States national seismic Hazard maps. *Report*, 1091, 243. <https://doi.org/10.3133/ofr20141091>
- Rice, J. R. (2006). Heating and weakening of faults during earthquake slip. *Journal of Geophysical Research*, 111(B5), B05–B311. <https://doi.org/10.1029/2005JB004006>
- Rogers, G., & Dragert, H. (2003). Episodic tremor and slip on the Cascadia subduction zone: The chatter of silent slip. *Science*, 300(5627), 1942–1943. <https://doi.org/10.1126/science.1084783>
- Rolandone, F., Nocquet, J.-M., Mothes, P. A., Jarrin, P., Vallée, M., Cubas, N., et al. (2018). Areas prone to slow slip events impede Earthquake rupture propagation and promote afterslip. *Science Advances*, 4(1), eaao6596. <https://doi.org/10.1126/sciadv.aao6596>
- Romanet, P., Bhat, H. S., Jolivet, R., & Madariaga, R. (2018). Fast and slow slip events emerge due to fault geometrical complexity. *Geophysical Research Letters*, 45(10), 4809–4819. <https://doi.org/10.1029/2018GL077579>
- Romanet, P., & Ozawa, S. (2021). Fully dynamic Earthquake cycle simulations on a nonplanar fault using the spectral Boundary Integral Element Method (sBIEM). *Bulletin of the Seismological Society of America*, 112(1), 78–97. <https://doi.org/10.1785/0120210178>
- Rousset, B., Bürgmann, R., & Campillo, M. (2019). Slow slip events in the roots of the San Andreas Fault. *Science Advances*, 5(2), eaav3274. <https://doi.org/10.1126/sciadv.aav3274>
- Royer, A. A., Thomas, A. M., & Bostock, M. G. (2015). Tidal modulation and triggering of low-frequency Earthquakes in Northern Cascadia. *Journal of Geophysical Research: Solid Earth*, 120(1), 384–405. <https://doi.org/10.1002/2014JB011430>
- Ruiz, S., & Madariaga, R. (2018). Historical and recent large megathrust earthquakes in Chile. *Tectonophysics*, 733, 37–56. <https://doi.org/10.1016/j.tecto.2018.01.015>
- Ruiz, S., Metois, M., Fuenzalida, A., Ruiz, J., Leyton, F., Grandin, R., et al. (2014). Intense foreshocks and a slow slip event preceded the 2014 Iquique Mw 8.1 Earthquake. *Science*, 345(6201), 1165–1169. <https://doi.org/10.1126/science.1256074>
- Saillard, M., Audin, L., Rousset, B., Avouac, J.-P., Chlieh, M., Hall, S. R., et al. (2017). From the seismic cycle to long-term deformation: Linking seismic coupling and quaternary coastal geomorphology along the Andean megathrust. *Tectonics*, 36(2), 241–256. <https://doi.org/10.1002/2016TC004156>
- Saux, J. P., Molitors Bergman, E. G., Evans, E. L., & Loveless, J. P. (2022). The role of slow slip events in the Cascadia subduction zone Earthquake cycle. *Journal of Geophysical Research: Solid Earth*, 127(2), e2021JB022425. <https://doi.org/10.1029/2021JB022425>
- Schwartz, S. Y., & Rokosky, J. M. (2007). Slow slip events and seismic tremor at circum-pacific subduction zones. *Reviews of Geophysics*, 45(3), RG3004. <https://doi.org/10.1029/2006rg000208>
- Segall, P., & Bradley, A. M. (2012). Slow-slip evolves into megathrust earthquakes in 2D numerical simulations. *Geophysical Research Letters*, 39(18), L18308. <https://doi.org/10.1029/2012GL052811>
- Segall, P., & Rice, J. R. (1995). Dilatancy, compaction, and slip instability of a fluid-infiltrated fault. *Journal of Geophysical Research*, 100(B11), 22155–22171. <https://doi.org/10.1029/95JB02403>

- Segall, P., Rubin, A. M., Bradley, A. M., & Rice, J. R. (2010). Dilatant strengthening as a mechanism for slow slip events. *Journal of Geophysical Research*, 115(B12), B12305. <https://doi.org/10.1029/2010JB007449>
- Shelly, D. R., Beroza, G. C., & Ide, S. (2007). Complex evolution of transient slip derived from precise tremor locations in Western Shikoku, Japan. *Geochemistry, Geophysics, Geosystems*, 8(10), Q10014. <https://doi.org/10.1029/2007GC001640>
- Sibson, R. H. (1973). Interactions between temperature and pore-fluid pressure during earthquake faulting and a mechanism for partial or total stress relief. *Nature*, 243(126), 66–68. <https://doi.org/10.1038/physci243066a0>
- Simons, M., Minson, S. E., Sladen, A., Ortega, F., Jiang, J., Owen, S. E., et al. (2011). The 2011 magnitude 9.0 Tohoku-Oki Earthquake: Mosaicking the megathrust from seconds to centuries. *Science*, 332(6036), 1421–1425. <https://doi.org/10.1126/science.1206731>
- Tanaka, Y., Yabe, S., & Ide, S. (2015). An estimate of tidal and non-tidal modulations of plate subduction speed in the transition zone in the Tokai district. *Earth Planets and Space*, 67(1), 141. <https://doi.org/10.1186/s40623-015-0311-2>
- Tanikawa, W., & Shimamoto, T. (2009). Frictional and transport properties of the Chelungpu fault from shallow borehole data and their correlation with seismic behavior during the 1999 Chi-Chi Earthquake. *Journal of Geophysical Research*, 114(B1), B01402. <https://doi.org/10.1029/2008JB005750>
- Tsutsumi, A., & Shimamoto, T. (1997). High-velocity frictional properties of gabbro. *Geophysical Research Letters*, 24(6), 699–702. <https://doi.org/10.1029/97GL00503>
- Ulrich, T., Gabriel, A. A., Ampuero, J. P., & Xu, W. (2019). Dynamic viability of the 2016 Mw 7.8 Kaikoura Earthquake cascade on weak crustal faults. *Nature Communications*, 10(1), 1213. <https://doi.org/10.1038/s41467-019-10912-w>
- Wibberley, C. A. J., Yielding, G., & Toro, G. D. (2008). Recent advances in the understanding of fault zone internal structure: A review, in the internal structure of Fault zones: Implications for mechanical and fluid-flow properties. *Geological Society of London*, 299(1), 5–33. <https://doi.org/10.1144/SP299.2>
- Wirth, E. A., & Frankel, A. D. (2019). Impact of down-dip rupture limit and high-stress drop subevents on coseismic land-level change during Cascadia Megathrust Earthquakes. *Bulletin of the Seismological Society of America*, 109(6), 2187–2197. <https://doi.org/10.1785/0120190043>
- Yin, J., & Denolle, M. A. (2021). The earth's surface controls the depth-dependent seismic radiation of megathrust earthquakes. *AGU Advances*, 2(3), e2021AV000413. <https://doi.org/10.1029/2021AV000413>